Separation Science and Technology
Publication details, including instructions for authors and subscription information:
http://www.informaworld.com/smpp/title~content=t713708471

Suction effect on the shear stress at a plane ultrafiltration ceramic membrane surface

C. Gaucher[a]; P. Jaouen[a]; P. Legentilhomme[a]; J. Comiti[a]
[a] Bd de l'Université, Saint-Nazaire cedex, France

Online publication date: 07 June 2002

To cite this Article Gaucher, C. , Jaouen, P. , Legentilhomme, P. and Comiti, J.(2002) 'Suction effect on the shear stress at a plane ultrafiltration ceramic membrane surface', Separation Science and Technology, 37: 10, 2251 — 2270
To link to this Article: DOI: 10.1081/SS-120003512
URL: http://dx.doi.org/10.1081/SS-120003512

SEPARATION SCIENCE AND TECHNOLOGY, 37(10), 2251–2270 (2002)

SUCTION EFFECT ON THE SHEAR STRESS AT A PLANE ULTRAFILTRATION CERAMIC MEMBRANE SURFACE

C. Gaucher, P. Jaouen, P. Legentilhomme,* and J. Comiti

GEPEA, Laboratoire de Génie des Procédés—
Environnement Agroalimentaire, UMR-MA 100, CRTT,
Bd de l'Université, BP 406, 44602 Saint-Nazaire cedex,
France

ABSTRACT

Wall shear stresses are determined at the surface of a plane ceramic ultrafiltration membrane using an electrochemical method. Twenty microelectrodes are mounted flush to this ceramic membrane and maps of shear stress and turbulent intensity rate are determined for three inlet/outlet distributors configurations. The experimental results are compared to that obtained previously in the same configurations without permeation. Thus, the wall shear rates and the turbulent intensity rates obtained with a transmembrane pressure of 50 kPa and a ratio of the permeation Reynolds number (more commonly called wall Reynolds number) to the channel Reynolds numbers, Re_w/Re, ranged between 1.3×10^{-5} and 6.4×10^{-4}, show the influence of the permeation on the velocity profile at the wall of a plane channel. Furthermore, the suction effect induces a softening of the

*Corresponding author. E-mail: legenti@gepea.univ-nantes.fr

incidence of the inlet/outlet configurations. Indeed, the average wall shear rate value is 15,000 $\sec^{-1}$ and the average turbulent intensity rate value is about 15% for the three distributors investigated.

INTRODUCTION

Crossflow ultrafiltration is a widely used technique for phases separation of many types of solutions and suspensions. Generally, the flow is driven by a pressure difference between the retentate and permeate sections of the separation module. As the bulk flows over the porous membrane, solvent (with components smaller than the size of the pores) flows through the membrane. Larger particles and solutes accumulate at the membrane surface to form a layer. This phenomenon is usually called membrane fouling. The most serious operational problem in industrial processes is the flux decline with time due to this membrane fouling. Some experimental evidence, available in the literature, shows that the effective parameter for the characterization of the crossflow transport in membrane separation processes is not the mean crossflow velocity nor the Reynolds number, but the wall shear stress (1,2). Different mechanisms have been reported to be responsible for the erosion phenomenon (3). All these approaches include a major controlling parameter, the wall shear stress at the membrane surface. Wall shear stress can be related, through the fluid velocity, to the mass transfer coefficient, and it could therefore be a useful parameter to investigate the fouling process. Indeed, many ultrafiltration models provide a relationship between the permeation flux and the mass transfer coefficient (4,5).

The study of wall suction effects on the structure of the flow in a plane channel has both practical and theoretical interest. Flow in a plane channel with mass withdrawal from the wall (i.e., suction) is encountered in a variety of ultrafiltration processes, and it is well known that wall suction has a significant effect on mass, momentum, and heat transfer rates. From a theoretical point of view, wall suction, even at low rates, affects the near-wall mean velocities and induces an alteration of the logarithmic velocity law at the wall. In addition, it increases the wall shear stress in the suction region and reduces the turbulence levels. Indeed, Sofialidis and Prinos (6) studied numerically the effects of wall suction on the structure of fully developed pipe flow, by solving the Reynolds averaged Navier–Stokes equations. Linear and nonlinear $k-\varepsilon$ or $k-\omega$ low-Re models of turbulence are used for "closing" the system of the governing equations. Computed results are compared

satisfactorily with experimental measurements obtained by Schildknecht et al. (7). Thus, they showed that wall suction tends to decrease the levels of the turbulent shear stress, indicating that reverse transition from turbulent to laminar flow would take place for a longer suction length. Furthermore, increased boundary shear stress along the suction region is calculated. The increase in wall shear stress is significant (up to 50%) even for the smallest suction rate ($4.6 \times 10^{-3} < Re_w/Re < 2.5 \times 10^{-2}$).

Concerning the effect of wall suction in a plane channel, to our knowledge, only numerical studies are available in the literature. For instance, Yucel and Turkoglu (8) have studied the Newtonian, incompressible, and viscous laminar flow of a solution between two parallel plates, the bottom plate being a permeable porous wall, while the top one is impermeable. The flow is driven by a pressure gradient. For an inlet Reynolds number equal to 2000, various wall Reynolds numbers ($0.1 < Re_w < 0.3$) and various tangential wall velocities were investigated. Indeed, Beavers and Joseph (9) proved the existence of a nonzero tangential velocity (slip) on the surface of a permeable boundary. Thus, Yucel and Turkoglu (8) concluded that, for the same wall nonzero tangential velocity, since the suction rate in tangential membrane filtration systems is very small compared with the axial resulting velocity ($5 \times 10^{-5} < Re_w/Re < 1.5 \times 10^{-4}$), a change in the suction velocity does not affect the behavior of the flow to any considerable extent. However, it should be emphasized that the change of the wall tangential velocity value plays an important role in the flow behavior. Zhapbasbaev and Isakhanova (10) have investigated numerically the turbulent flow in a plane channel with porous walls. For a permeation Reynolds number (Re_w) equal to zero, the velocity profile is symmetric about the central plane of the channel. When the wall Reynolds number increases ($0 < Re_w < 1.6 \times 10^2$), a deformation of the velocity profile is observed. The distribution of the velocity becomes asymmetric about the central plane, levels out near the wall where injection occurs, and, conversely, fills out near the wall where suction occurs. Thus, the wall Reynolds number does not drastically affect the mean velocity in the channel, but induces a deformation of the velocity profile at the porous wall, changing the wall tangential velocity value.

In our previous works, the influence of the channel height and of the inlet/outlet configurations (11) and the incidence of the design of the distributors (12) on the wall shear stress have been studied at the surface of a plate of Plexiglas (without permeation) in a plane ultrafiltration module, using an electrochemical method. The aim of the present work is to investigate the influence of the suction velocity on the behavior of the wall shear stress at a plane ceramic membrane surface, using an electrochemical method.

THEORY

The experimental determination of shear stress at the surface of a plane ceramic ultrafiltration membrane is made using an electrochemical method based on the reduction of the ferricyanide ion on a cathodic surface:

$$Fe(CN)_6^{3-} + e^- \rightarrow Fe(CN)_6^{4-}$$

The reverse reaction takes place at the anode.

Under diffusion-controlled conditions on the microelectrodes, the mass transfer coefficient, k, between the electrolyte and the probe surface is related to the limiting diffusional current, I_L, by:

$$I_L = \nu_e F \frac{\pi d_e^2}{4} C_0 k \tag{1}$$

where ν_e is the number of electrons involved in the electrochemical reaction ($\nu_e = 1$), F is the Faraday's constant, d_e is the electrode diameter, and C_0 the bulk concentration of the ferricyanide ions.

We consider a circular probe embedded flush to a solid wall. The diameter, d_e, of this circular probe is small enough to neglect the effect of the normal velocity component.

In addition, we consider situations such that $\bar{S}d_e^2/D$ is larger than 5000 in order to neglect diffusion in the direction of the mean flow (coordinate x) as shown by Ling (13). Owing to the above mentioned consideration that the dimensions in the x- and z-directions are the same for a circular probe, we assume that both $\partial^2 c/\partial z^2$ and $\partial^2 c/\partial x^2$ can be neglected.

Thus, at stationary state, the convection–diffusion equation becomes:

$$\bar{U}\frac{\partial c}{\partial x} = D\frac{\partial^2 c}{\partial y^2} \tag{2}$$

where D is the diffusion coefficient of the transferred species.

Furthermore, the thickness of the mass boundary layer is small compared with that of the hydrodynamical boundary layer ($Sc = 1000$), so the viscous boundary layer has some linear properties and $\bar{U} = \bar{S}y$ can be assumed (14).

Equation (2) has been solved by Reiss and Hanratty (14) and Mitchell and Hanratty (15) for rectangular and circular microprobes. When circular microelectrodes are embedded in an inert wall, the mass transfer coefficient is related to the mean wall velocity gradient, $\bar{S}$, in steady-state conditions by (14):

$$k = 0.862\left(\frac{D^2\bar{S}}{d_e}\right)^{1/3} \tag{3}$$

Combining Eqs. (1) and (3), the wall velocity gradient can be determined and then the wall shear stress can be calculated by:

$$\tau = \mu \bar{S} \tag{4}$$

where μ represents the dynamic viscosity of the electrolytic solution.

The electrode length is very small compared to the membrane length, thus, a developing diffusional boundary layer of small thickness exists at the electrode surface, which acts as a filter, dumping the fluctuations of the wall velocity gradient. The diffusion coefficient of the ferricyanide ions and the electrode diameters are needed to obtain wall shear stress values. The diffusion coefficient is measured by a classical method using a rotating disc electrode and the electrode diameter using a voltage-step transient technique (16). This method is based on the study of the transient response of the electrodes to a voltage step from zero to the diffusional plateau potential. This calibration is interesting for electrodes located inside the module because it can be carried out in real experimental conditions. Moreover, it does not require any knowledge of local hydrodynamics.

The turbulent intensity rate, T_s, defined by Eq. (5), is used to quantify the velocity gradient fluctuations:

$$T_s = \frac{\sqrt{\overline{s^2}}}{\bar{S}} \tag{5}$$

where s represents the fluctuating velocity gradient and $\bar{S}$ the mean velocity gradient, following the decomposition:

$$S(t) = \bar{S} + s(t) \quad \text{with } \overline{s(t)} = 0 \tag{6}$$

The velocity gradient fluctuations are filtered by the diffusional boundary layer at the active surface (17). To take this phenomenon into account, the electrochemical transfer function, $H(f)$, between the diffusional current and the velocity gradient at the electrode must be determined. This function links the power spectral density at frequency f of the diffusional current fluctuation, $W_{ii}(f)$, and that of the power spectral density of the velocity gradient, $W_{ss}(f)$:

$$W_{ii}(f) = |H(f)|^2 W_{ss}(f) \tag{7}$$

where $|H(f)|$ is the amplitude of the transfer function (18).

This turbulent intensity rate is calculated by integrating the velocity gradient power density spectrum, $W_{ss}(f)$:

$$T_s = \frac{\sqrt{2\int_0^{\infty} W_{ss}(f)\mathrm{d}f}}{\bar{S}} \approx \frac{\sqrt{2\int_0^{f_c} W_{ss}(f)\mathrm{d}f}}{\bar{S}} \tag{8}$$

where f_c is the upper bound of the integration of the power density spectrum.

MATERIALS AND METHOD

The electrolytic solution was thermostated at 30°C in the feed tank. The fluid is brought to the circuit by a centrifugal-type pump to ensure a constant tangential velocity at the plane surface. The flow rates are measured using a rank of two flowmeters. The filtration could be conducted under constant differential pressure conditions of 50 kPa, using a second pump and a pressure throttling valve installed on the outlet side of the membrane module. The permeate and the retentate are returned to the feed tank to keep a constant concentration of particles during ultrafiltration process.

The crossflow ultrafiltration apparatus, used in industrial processes (19), has internal dimensions of 122 mm length and width, and a 1 mm channel height. The fluid enters through different distributors described in a previous work (12), and then flows tangentially to the plane plate. The membrane used is an ultrafiltration ceramic plane membrane commercialized by Tami Industrie (Nyons, France). The membrane molecular weight cut-off (given by the manufacturer) is 150 kDa. The interest of the ceramic membrane plate is to offer to the end user both the advantages of ceramic material and flat geometry. The main advantages are the equipment modularity, the easiness for sanitation, the reduction of energy consumption and equipment costs, and the good resistance at extreme pH and high temperatures (19).

Twenty microelectrodes are mounted flush to the membrane. A nickel anode is inserted at the top of the module. The microelectrodes are made of a platinum wire 0.4 mm in diameter. A potential of -400 mV is applied between the anode and the cathode in order to ensure limiting diffusional conditions at the microelectrodes surface (diffusional limiting plateau).

Experimental data are stored on a digital audio tape (DAT) and transferred to a computer to be analyzed by means of the signal processing software LABVIEW. For each Reynolds number at stationary state, the limiting current is recorded during one minute and the local wall shear stress considered further is an average of all the values recorded during this time.

The electrolytic solution is a mixture of potassium ferricyanide ($2\,\mathrm{mol\,m^{-3}}$), potassium ferrocyanide ($50\,\mathrm{mol\,m^{-3}}$), and potassium sulfate

($100\,\mathrm{mol\,m^{-3}}$). The potassium sulfate acts as a low resistance vehicle for current flow and ensures that the transfer at the cathodic surface is only controlled by diffusion. At a working temperature of 30°C, the diffusion coefficient of the ferricyanide ions is $8.36 \times 10^{-10}\,\mathrm{m^2\,sec^{-1}}$, the density is $1023\,\mathrm{kg\,m^{-3}}$ and the kinematic viscosity is $0.815 \times 10^{-6}\,\mathrm{m^2\,sec^{-1}}$.

The channel Reynolds number is defined by:

$$Re = \frac{U_0 d_H}{\nu} \tag{9}$$

and the permeation (or wall) Reynolds number is defined by:

$$Re_w = \frac{J_{lim} d_H}{\nu} \tag{10}$$

where $d_H = 2e$ (e is the channel height), U_0 is the mean velocity in the channel defined by:

$$U_0 = \frac{Q}{Le} \tag{11}$$

where Q represents the volumic flow rate and L the length of the module. J_{lim} is the permeation velocity through the porous wall defined by:

$$J_{lim} = \frac{P_{TM}}{\mu R_m} = \frac{Q_w}{L^2} \tag{12}$$

where P_{TM}, μ, R_m, and Q_w are respectively the transmembrane pressure, the dynamic viscosity, the hydraulic membrane resistance, and the volumic permeation flow rate measured during the experiments.

The channel Reynolds number is varied from 100 to 3470, while the wall Reynolds number is ranged between 1.3×10^{-5} and 6.4×10^{-4}.

RESULTS AND DISCUSSION

As the knowledge of the electrode diameters is needed in order to determine the local wall velocity gradient, a calibration of the microprobes is carried out. Ten experiments have been performed for each probe. The results are given in Table 1. The electrode diameter values are close to the platinum wire diameter ($400\,\mu$m), the difference is due to the various operations needed for their implementation at the membrane surface.

The local wall shear stresses are determined for a Reynolds number of 3470 and for three designs of distributors described in Table 2. These three distributors have been chosen according to three different criterions. First, these inlet/outlet configurations have a ratio of the inlet velocity to the mean

Table 1. Calibration of the Microelectrodes

Microprobe	d_e (μm)	Standard Deviation (μm)	$(\lvert d_e - d_{wire}\rvert / d_{wire}) \times 100$ (%)
1	319	16	20
2	357	8	11
3	443	6	11
4	425	27	6
5	387	15	3
6	370	22	8
7	258	12	35
8	456	8	14
9	393	10	2
10	327	8	18
11	387	8	3
12	450	8	12
13	374	18	7
14	358	19	10
15	344	23	14
16	465	21	16
17	390	6	2
18	405	5	1
19	380	10	5
20	444	10	11

tangential one inducing a deceleration or an acceleration of the mean tangential velocity in the module (Table 3). Secondly, they induce different wall shear rates at the surface of the plane plate without suction (12) (Table 3). Thirdly, they induce low-pressure drops (Table 3). Figure 1 represents the wall shear stress values versus the electrodes position on the membrane (with $P_{TM} = 50$ kPa) or on the plate of Plexiglas (12) without suction, for the three distributors configurations. Without suction, two zones of low shear stress near the module walls and a zone of high shear stress in the middle of the plate can be observed. Applying a transmembrane pressure of 50 kPa induces a better homogeneity of the wall shear stress values at the membrane surface, with a small zone of very high shear stress near the module outlet. To compare this homogeneity of wall shear stress at the membrane surface without the zone with very high shear stress, the ratios of the standard deviation and the mean wall velocity gradient were calculated without the probes 1, 2, and 10. These ratios are between 0.57 and 0.67 for the experiments realized with a suction effect and between 0.69 and 0.84 for the

Table 2. Description of the Different Distributors Investigated

Distributors Shape	Description	S_{inlet}/S_{module}
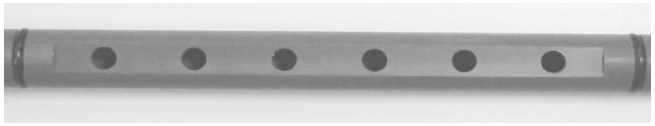	Six distributors of same diameter ($d = 6$ mm)	1.39
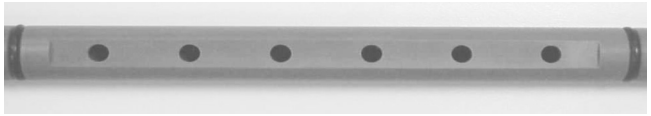	Six distributors of same diameter ($d = 5$ mm)	0.97
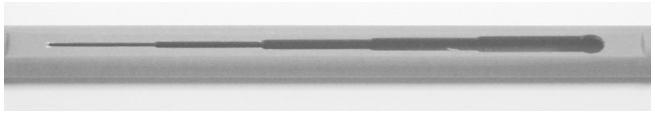	Distributor of "pseudo trapezoidal" shape	0.47

Table 3. Criteria of Selection of the Three Inlet/Outlet Configurations and Average Wall Shear Rates with or without Permeation—$Re = 3470$

	$\bar{S}$ (sec^{-1})	ΔP (kPa)	$U_{inlet}/U_{tangential}$	$\bar{S}$ without Suction (sec^{-1})	$\bar{S}$ with $P_{TM} = 50$ kPa (sec^{-1})
Six distributors of same diameter (6 mm)	7,811	12.5	0.72 (Acceleration)	7,811	15,116
Six distributors of same diameter (5 mm)	6,043	15	1.03	6,043	14,948
Distributor of trapezoidal shape	10,432	10	2.13 (Deceleration)	10,432	15,173

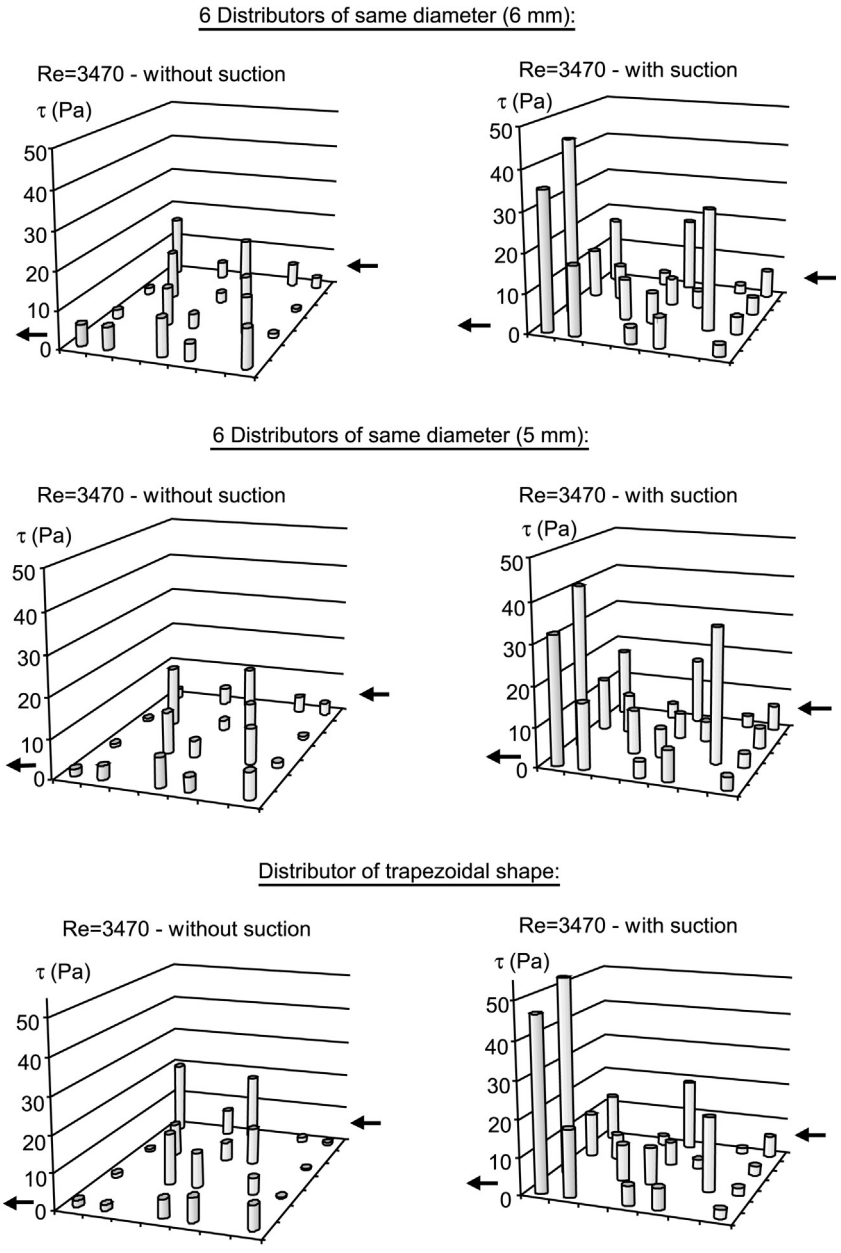

Figure 1. Local wall shear stress vs. the electrode position for three inlet/outlet configurations, with or without suction—$Re = 3470$.

experiments realized without permeation. This phenomenon is common for the three distributors configurations.

The values of the wall velocity gradient for the three configurations with or without permeation and for a Reynolds number of 3470 are given in Table 3. The calculation of an average wall shear rate value on the 20 microelectrodes is necessary in order to obtain a comparable global character. In our previous work (12), the wall shear rate values obtained for the three configurations investigated are different, and it has been observed that greater the ratio between the inlet velocity and the mean one in the module, higher is the wall shear rate. In this work, when a transmembrane pressure of 50 kPa is applied, the difference of the local wall velocity gradient values vanishes (Fig. 2) and a mean wall velocity gradient value of 15,000 $\sec^{-1}$ is obtained for the three designs of distributors. The effect of the permeation flow is not insignificant regarding the wall velocity gradient as it was shown by Zhapbasbaev and Isakhanova (10), although the suction velocity is very low compared to the mean tangential velocity. Table 4 gives the different channel Reynolds numbers and wall Reynolds numbers for the three configurations investigated and those found in the literature. Yucel and Turkoglu (8) predicted that the suction effect does not affect the behavior of the flow to any considerable extent, but the value of the tangential wall velocity plays an important role. Indeed the mean flow is probably not drastically changed, our results show that the suction velocity influences the tangential wall velocity and the influence of the distributors design seems to disappear.

Figure 3 presents the evolution of the ratio of the average wall shear rate with suction and the wall shear rate without suction (12) vs. the ratio of the wall Reynolds number and the axial Reynolds number. The ratio of wall velocity gradients is constant for the configuration with six distributors of 5 mm in diameter and increase for the configurations with six distributors of 6 mm and that of trapezoidal shape. Thus, the permeation Reynolds number being constant, the ratio of wall shear rates increases with the decrease of the channel Reynolds number for the configurations with six distributors of 6 mm and that of trapezoidal shape. For the configuration with six distributors of 5 mm in diameter (inducing no acceleration nor deceleration of the mean tangential velocity), the ratio of wall velocity gradients is constant for all the ratios of Reynolds numbers. Figure 2 shows wall velocity gradients with suction 1.5–2.5 times higher than those without suction. These results confirm the Zhapbasbaev and Isakhanova's ones (10), which show an increase of the wall tangential velocity (so, an increase of the wall shear rate compared with this obtained without suction) when the ratio of Reynolds numbers increases. Furthermore, Sofialidis and Prinos (6) found wall shear stresses with suction 1.5–5.5 times higher than those without permeation, and Herath et al. (20) measured mass transfer coefficients 2.5 times higher than those calculated using the Sherwood correlation based on Chilton–Colburn analogy ($Sh = 0.023Re^{0.8}Sc^{0.33}$) without permeation.

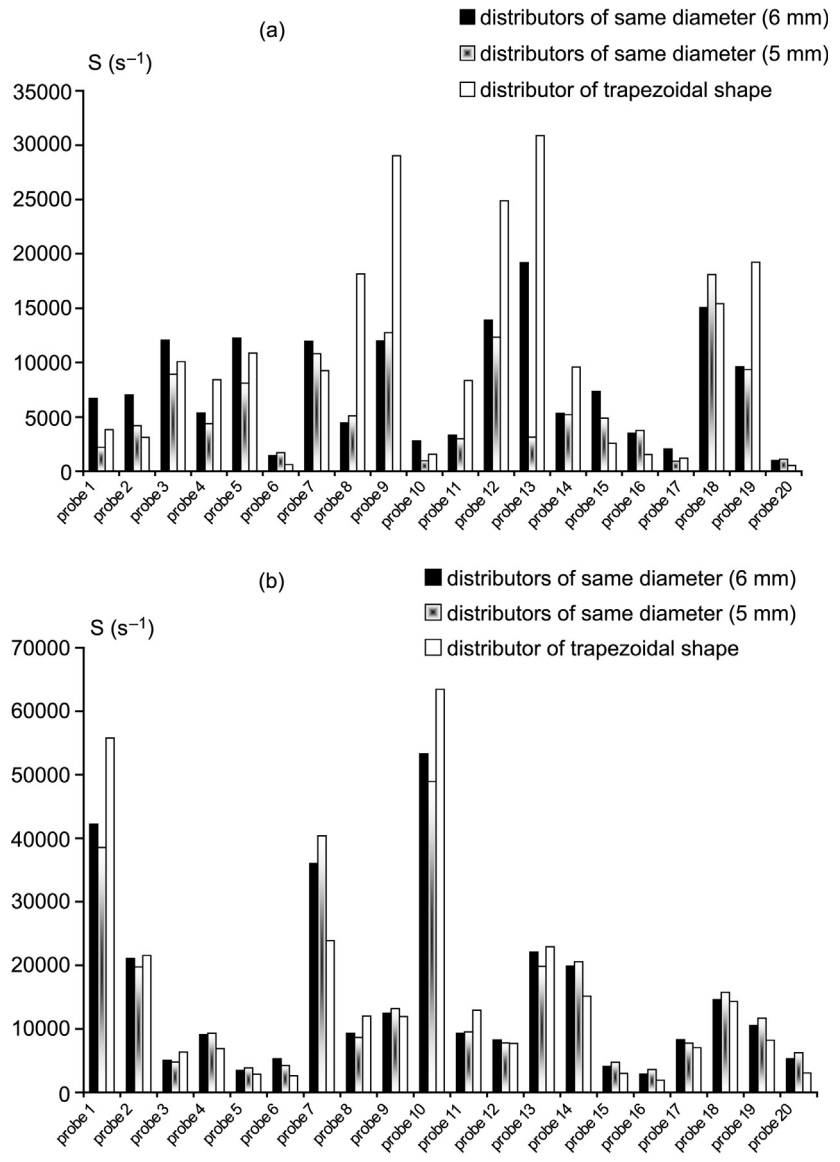

Figure 2. Comparison of the homogeneity of the local wall shear rates obtained with (b) or without (a) permeation—$Re = 3470$.

Table 4. Comparison of Our Experimental Reynolds Numbers to Those Found in the Literature

	$Re_w = (J_{lim} \times 2e)/\nu$	$Re = (U_0 \times 2e)/\nu$	Re_w/Re
6×6 mm	0.049	$100 < Re < 3470$	$1.4 \times 10^{-5} < Re_w/Re < 4.9 \times 10^{-4}$
6×5 mm	0.046	$100 < Re < 3470$	$1.3 \times 10^{-5} < Re_w/Re < 4.6 \times 10^{-4}$
Trapezoidal shape	0.064	$100 < Re < 3470$	$1.9 \times 10^{-5} < Re_w/Re < 6.4 \times 10^{-4}$
Yucel and Turkoglu (8)	$0.1 < Re_w < 0.3$	2000	$5 \times 10^{-5} < Re_w/Re < 1.5 \times 10^{-4}$
Zhapbasbaev and Isakhanova (10)	$0 < Re_w < 1.6 \times 10^2$	$16{,}000 < Re < 160{,}000$	$0 < Re_w/Re < 10^{-2}$
Sofialidis and Prinos (6) Schildknecht et al. (7)			4.6×10^{-3} and 2.53×10^{-2}

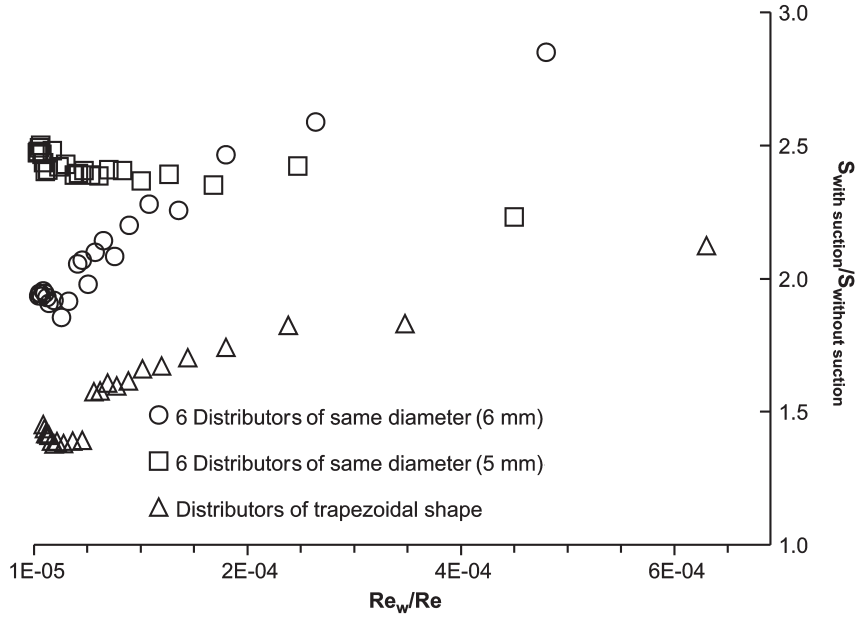

Figure 3. Ratio of average velocity gradient with permeation and average velocity gradient without permeation vs. Reynolds number.

Figure 4 represents the map of turbulent intensity rate of the velocity gradient for the three studied distributors with or without permeation. As it was previously described (11), the turbulent intensity rate obtained by the electrochemical method has been corrected using a ratio determined by Deslouis et al. (21) for measurements in a plane channel. Indeed, an electrode length larger than the size of the smallest eddies can have a significant effect on measurements of the fluctuating velocity gradient made with mass transfer probes. Thus, a ratio between the fluctuating measured velocity and the real fluctuating velocity is determined using the integral correlation length in the direction perpendicular to the flow (22). The turbulent intensity rates obtained without permeation (12) are higher near the module walls and near the inlet/outlet sections; this is mainly due to the wall effects that cause a higher turbulence level. The turbulent intensity rates obtained with permeation are more homogeneous; no different zones can be observed. The average turbulent intensity rate with permeation is two times lower than that obtained without permeation. Indeed, the average fluctuating velocity gradient values with permeation are about 15% for the three configurations, and the average turbulent intensity rates were about 25–30% without permeation (12). Thus, it seems that the suction velocity stabilizes the wall velocity gradient,

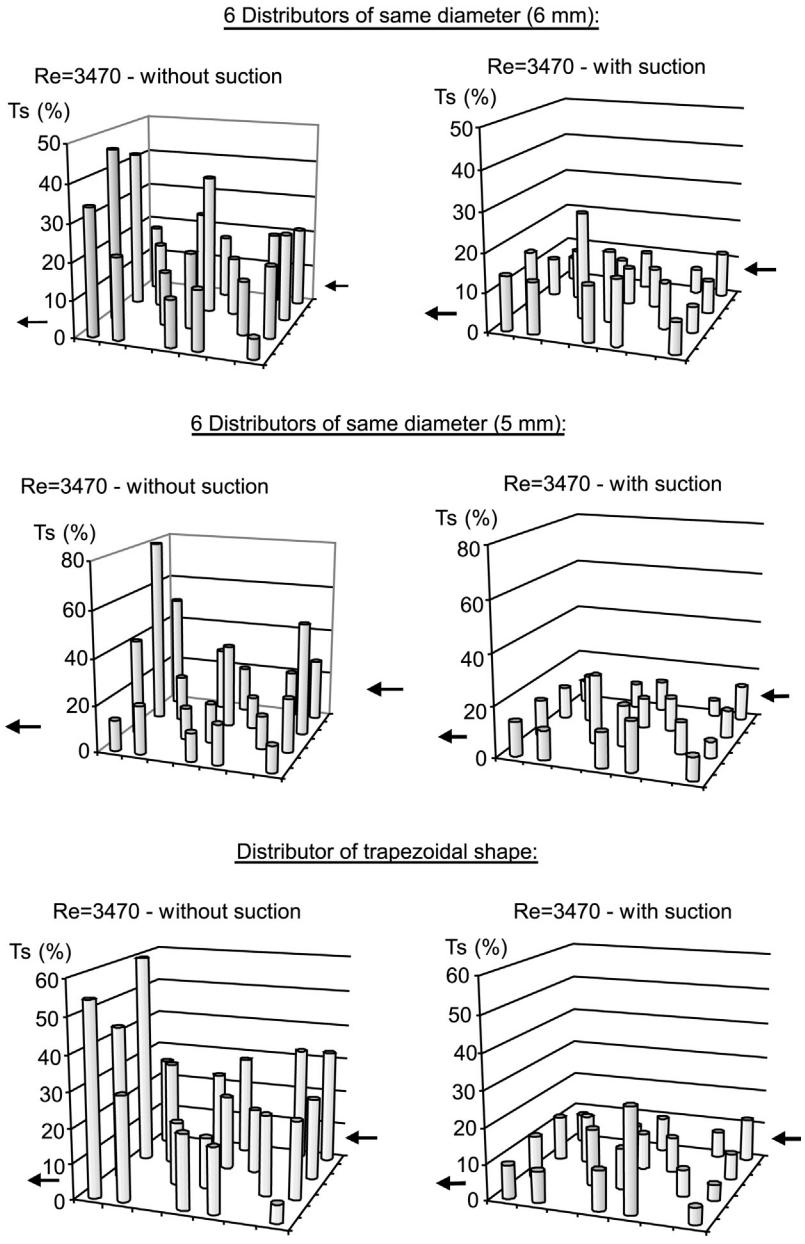

Figure 4. Local fluctuating rate of velocity gradient vs. the electrode position for three inlet/outlet configurations, with or without permeation—$Re = 3470$.

decreasing and homogenizing the fluctuations. These results are in the same range of Zhapbasbaev and Isakhanova (10) who found, numerically, a root-mean square value of the wall velocity fluctuations of about 10% with suction and about 30% without suction.

CONCLUSION

The comparison of the wall shear stress and the turbulent intensity rate determined at the surface of a plane ceramic ultrafiltration membrane (with permeation) and at the surface of a plane plate of Plexiglas (without permeation) show the influence of the suction velocity. Indeed, if the wall shear rates are different according to the fluid distribution at a plane plate surface without permeation, this difference vanishes when a transmembrane pressure is applied. Furthermore, the heterogeneity of the wall shear stress decreases when a transmembrane pressure of 50 kPa is applied. The flow at the wall is stabilized, and the inlet/outlet configurations do not change the wall tangential velocity radically.

Experimental results concerning the incidence of the suction exist only for developed pipe flow. Concerning the flow in a plane channel, only numerical results can be found in the literature. In this work, the electrochemical method allows wall measurements, and local wall shear stress values can be obtained. These experimental results confirm those obtained numerically by Yucel and Turkoglu (8) and Zhapbasbaev and Isakhanova (10), showing the incidence of the suction on the tangential velocity profile at a plane membrane surface.

This study has been performed with a transmembrane pressure of 50 kPa. It will be interesting to realize experiments using a greater transmembrane pressure to investigate the influence of the increase of the suction effect on the wall shear rate at the membrane surface.

NOMENCLATURE

C_o	bulk concentration (mol m^{-3})
d_e	electrode diameter (m)
d_H	hydraulic diameter of the cell (m)
D	diffusion coefficient of ferricyanide ions (m^2 sec^{-1})
e	channel height (m)
f	frequency (Hz)
f_c	upper bound of integration of the fluctuating velocity gradient (Hz)
F	Faraday's constant ($F = 96,500$ C mol^{-1})
I_L	limiting diffusional current (A)

J_{lim}	permeation velocity ($m\,sec^{-1}$)
k	mass transfer coefficient ($m\,sec^{-1}$)
L	channel length (m)
P_{TM}	transmembrane pressure (Pa)
Q	volumic flow rate ($m^3\,sec^{-1}$)
Q_w	permeation flow rate ($m^3\,sec^{-1}$)
Re	channel Reynolds number
Re_w	wall Reynolds number (or permeation Reynolds number)
R_m	hydraulic resistance (m^{-1})
$S(t)$, $\bar{S}$, $s(t)$	instantaneous, average, and fluctuating velocity gradients (sec^{-1})
S_{module}	module section ($S_{module} = L \times e$) (m^2)
S_{inlet}	section of the distributors (m^2)
T_s	turbulent intensity rate
$\bar{U}$	mean velocity component in the flow direction ($m\,sec^{-1}$)
U_0	mean velocity in the cell ($m\,sec^{-1}$)
W_{ii}	power spectral density of the fluctuating current ($A^2\,sec$)
W_{ss}	power spectral density of the velocity gradient (sec^{-1})

Greek Letters

μ	dynamic viscosity (Pa sec)
ν	kinematic viscosity ($m^2\,sec^{-1}$)
ν_e	number of electrons involved in the electrochemical reaction
ρ	density ($kg\,m^{-3}$)
τ	wall shear stress (Pa)

REFERENCES

1. Gésan-Guiziou, G.; Daufin, G.; Boyaval, E.; Le Berre, O. Wall Shear Stress: Effective Parameter for the Characterization of the Crossflow Transport in Turbulent Regime During Skimmed Milk Microfiltration. Lait **1999**, *79*, 347–354.
2. Grandison, A.S.; Youravong, W.; Lewis, M.J. Hydrodynamic Factors Affecting Flux and Fouling During Ultrafiltration of Skimmed Milk. Lait **2000**, *80*, 165–174.
3. Huisman, I.H.; Trägårdh, C. Particle Transport in Crossflow Microfiltration. I—Effects of Hydrodynamics and Diffusion. Chem. Eng. Sci. **1999**, *54*, 271–280.
4. Mickaels, A.S. New Separation Technique for the Chemical Process Industry. Chem. Eng. Sci. **1968**, *25*, 1429–1435.

5. Porter, M. Concentration Polarization with Membrane Ultrafiltration. Ind. Eng. Chem. Prod. Res. Dev. **1972**, *11*, 234–248.
6. Sofialidis, D.; Prinos, P. Wall Suction Effects on the Structure of Fully Developed Turbulent Pipe Flow. J. Fluid Eng. **1996**, *118*, 33–39.
7. Schildknecht, M.; Miller, J.A.; Meier, G.E.A. The Influence of the Suction on the Structure of Turbulence in Fully Developed Pipe Flow. J. Fluid Mech. **1979**, *90*, 67–107.
8. Yucel, N.; Turkoglu, H. Numerical Analysis of Fluid Flow and Mass Transfer in a Channel with a Porous Bottom Wall. Int. J. Num. Meth. Fluids **1995**, *21*, 391–399.
9. Beavers, G.S.; Joseph, D.D. Boundary Conditions at a Naturally Permeable Wall. J. Fluid Mech. **1967**, *30*, 197–207.
10. Zhapbasbaev, U.K.; Isakhanova, G.Z. Developed Turbulent Flow in a Plane Channel with Simultaneous Injection Through One Porous Wall and Suction Through the Other. Appl. Mech. Tech. Phys. **1998**, *39*, 53–59.
11. Gaucher, C.; Legentilhomme, P.; Jaouen, P.; Comiti, J.; Pruvost, J. Hydrodynamics Study in a Plane Ultrafiltration Module Using an Electrochemical Method and PIV Visualization. Exp. Fluids **2002**, *32*, 283–293.
12. Gaucher, C.; Legentilhomme, P.; Jaouen, P.; Comiti, J. Influence of Fluid Distribution on the Wall Shear Stress in a Plane Ultrafiltration Module Using an Electrochemical Method. Chem. Eng. Res. Des. **2002**, *80* (1), 111–120.
13. Ling, S.C. Heat Transfer from a Small Isothermal Span Wise Strip on an Insulated Boundary. Trans. Am. Soc. Mech. Eng. Series C, J. Heat Transfer **1963**, *85*, 230–236.
14. Reiss, L.P.; Hanratty, T.J. An Experimental Study of the Unsteady Nature of the Viscous Sublayer. AIChE J. **1963**, *9*, 154–160.
15. Mitchell, J.E.; Hanratty, T.J. A Study of Turbulence at a Wall Using an Electrochemical Wall Shear Stress Meter. J. Fluid Mech. **1966**, *26*, 199–221.
16. Sobolik, V.; Tihon, J.; Wein, O.; Wichterle, K. Calibration of Electrodiffusion Friction Probes Using a Voltage-Step Transient. J. Appl. Electrochem. **1998**, *28*, 329–335.
17. Lebouché, M. Contribution à l'étude des Mouvements Turbulents des Liquides par la Méthode Polarographique. Ph.D. Thesis, Nancy, France.
18. Nakoryakov, V.E.; Budukov, A.P.; Kashinsky, O.N.; Geshev, P.I. *Electrodiffusion Method of Investigation into the Local Structure of Turbulent Flows*; Gasenko, V.G., Ed.; 1986.
19. Grangeon, A.; Lescoche, P. Flat Ceramic Membranes for the Treatment of Dairy Products: Comparison with Tubular Ceramic Membranes. Lait **2000**, *80*, 165–174.

20. Herath, G.; Yamamoto, K.; Urase, T. The Effect of Suction Velocity on Concentration Polarization in Microfiltration Membranes Under Turbulent Flow Conditions. J. Membr. Sci. **2000**, *169*, 175–183.
21. Deslouis, C.; Huet, F.; Robin, S.; Tribollet, B. Spectral Analysis of Wall Turbulence with Photolithography Devised Electrochemical Probes. Int. J. Heat Mass Transfer **1993**, *36*, 823–829.
22. Uberoi, M.S.; Kovasznay, L.S.G. On Mapping and Measurement of Random Fields. Appl. Math. **1953**, *10*, 375–393.

Received September 2001
Revised December 2001